✱✱✱✱✱✱✱✱✱✱✱Accepted Manuscript✱✱✱✱✱✱✱✱✱✱

This article is an accepted manuscript

It has been peer reviewed and accepted for publication but has not yet been copyedited, house styled, proofread or typeset. The final published version may contain differences as a result of the above procedures

It will be published in the *Johnson Matthey Technology Review*

Please visit the website https://technology.matthey.com/ for Open Access to the article and the full issue once published

Editorial team

Manager Dan Carter
Editor Sara Coles
Editorial Assistant Yasmin Stephens
Senior Information Officer Elisabeth Riley

OPEN ACCESS

<https://doi.org/10.1595/205651323X16648726195503>

<First page number: TBC>

Advanced Supports for Noble Metal Catalysts in Proton Exchange Membrane Water Electrolysers: A Review

By Pere L. Cabot*

Laboratory of Electrochemistry of Materials and the Environment, Dep. of Materials Science and Physical Chemistry, Universitat de Barcelona, Martí i Franqués 1-11, 08028 Barcelona, Spain

María V. Martínez-Huerta

Instituto de Catálisis y Petroleoquímica, CSIC, C/ Marie Curie, 2. 28049 Madrid, Spain

Francisco Alcaide

Laboratory of Electrochemistry of Materials and the Environment, Dep. of Materials Science and Physical Chemistry, Universitat de Barcelona, Martí i Franqués 1-11, 08028 Barcelona, Spain

CIDETEC, Basque Research and Technology Alliance (BRTA), Po Miramón, 196, 20014 Donostia-San Sebastián, Spain

*Email: <p.cabot@ub.edu>

<ABSTRACT>

Renewable and low-carbon H_2 gas will contribute to a future climate neutral economy as a fuel, clean energy carrier and/or feedstock. One of the main concerns when considering its production by the present proton exchange membrane water electrolysis (PEMWE) is the use of scarce and expensive noble metals as catalysts for the hydrogen and oxygen evolution reactions, HER and OER, respectively, because they contribute to increase the cost of the technology. In this sense, several strategies have been developed to overcome this drawback, such as optimising the catalyst loading in the electrodes and alloying and/or using alternative catalyst supports, always with the aim to maintain or even increase the electrolyser performance and durability. In this review, we examine the latest developments in HER and OER catalysts intended for PEMWE practical systems, which point in the short term to the use of Pt and Ir noble-metal nanoparticles highly dispersed at low loadings on conductive non-carbon supports.

1. Introduction

The renewable energy sources have gained significant attention since many years ago due to the limited amounts of fossil fuels and their environmental impact on the Earth. The increasing release of CO_2, NO_x, heavy metals, ashes, tars and organic compounds from the combustion of fossil fuels to attend the energy demand of the planet has led to a rapid increase in the pollutants and greenhouse gases in the air (1)(2). Today, concerns about air pollution and climate change drive to seek for environmentally friendly, accessible, and economically attractive renewable energies as energy sources alternative to fossil fuels.

H_2 is the clean fuel of the future because water is the only product expected (although residual pollutants can appear depending on the purity of the fuel and the oxidizer). Pure H_2 disposal allows then obtaining clean energy (3). However, it is not available for direct use in the nature and therefore, it has to be produced (4). The current annual production is about 0.1 Gt, the most part being used for petroleum and metals refining (47%) and ammonia production (45%), whereas only a small fraction is applied for electronics fabrication, food industry and as fuel for transportation (5).

Nikolaidis and Poullikkas (4) have summarized the main advantages and disadvantages of the different methods of H_2 production. Steam reforming of hydrocarbons is the most developed one, with existing infrastructure, and efficiencies in the range 74-85%. Partial oxidation and autothermal steam reforming of hydrocarbons are proven technologies with smaller efficiencies in the range 60-75%. All these methods produce CO_2 as byproduct, depending on the fossil fuel. On the other hand, there are the methods using raw materials coming from renewable technologies,

namely biomass and water. The pyrolysis of biomass presents efficiencies of 35-50% and is CO_2-neutral, but its main disadvantages are the tar formation and the variable H_2 content depending on the seasonal availability and impurities of the feedstock. The dark fermentation of biomass has also good efficiencies in the range 60-80% and is CO_2-neutral, but its major disadvantages are the formation of fatty acids, which are organic pollutants that should be removed, low H_2 rates and yields and the need of large reactor volumes. Those utilizing water as the only raw material produce H_2 through water splitting processes such as electrolysis, thermolysis and photoelectrolysis. Thermolysis of water, with efficiencies in the range 20-45% is clean and sustainable, O_2 being also the only byproduct, but its major disadvantages are the toxicity of the elements used, corrosion problems and the need of high capital investment. Photoelectrolysis of water is also interesting since it is also free from emissions and O_2 is the only byproduct, but it requires sunlight, has efficiencies of about 0.06%, and suitable photocatalytic materials are needed. Conversely, electrolysis is a proven technology, with existing infrastructures and good efficiencies in the range 40-60%, with only O_2 as by-product. Although a high capital investment is required and the H_2 production by this method is still more expensive than that obtained from hydrocarbon reforming, water electrolysis appears as an environmentally friendly H_2 generation process and a key technique in the H_2 economy, which appears to be as a promising instrument for the transformation of the energy system.

Electrolysis is already today a basic technique to provide H_2 in small applications such as in food and semiconductor industry (5). Despite this, water electrolysis only

contributes with only about 4% in the overall H_2 production in the world (5). This can be significantly changed in the next decades since solar and wind renewable energy resources are expected to increase replacing fossil ones for environmental reasons. If the energy production by these methods exceeds the electricity demand, the energy storage as H_2 fuel can be a potential solution (1). This is particularly interesting because the renewable resources are intermittent and therefore, the exceeding energy in operation can be used in water electrolysis for H_2 production.

The alkaline electrolysis is the oldest and most mature technique, which uses a thin ceramic porous diaphragm submerged in the liquid alkaline electrolyte (6)(7)(8). There is also the possibility of using the anion exchange membrane technology in alkaline water electrolysis. However, this is quite a way from commercialisation. In the meantime, water electrolysis using proton exchange membrane water electrolysers (PEMWEs) is a recent and very attractive technique from an industrial viewpoint because it is a compact device of simple construction and flexible dynamic operation in which a proton exchange membrane (PEM) replaces the liquid electrolyte (9). Fig. 1 shows a schematic picture of a single cell of a PEMWE, as given in Ref. (10). The PEM is an acidic solid polymer electrolyte with very good proton conductivity (SPE in Fig. 1). Perfluorinated sulfonic-acid (PFSA) PEM membranes such as Nafion® ones are commonly used in the electrochemical technologies (11). The anode and the cathode reactions in the water electrolysis in acidic media are given by equations [1] and [2], OER and HER, respectively (3):

$$H_2O \rightarrow \frac{1}{2} O_2 + 2\ H^+ + 2\ e^- \tag{1}$$

$$2\ H^+ + 2\ e^- \rightarrow H_2 \tag{2}$$

The standard (reduction) electrode potentials are 1.23 and 0.00 V vs. SHE respectively and therefore, the standard Gibbs energy of the overall reaction [3], given by the summation of reactions [1] and [2]:

$$H_2O \rightarrow \frac{1}{2} O_2 + H_2 \qquad\qquad\qquad\qquad [3]$$

is $\Delta G^o = -2 \times 96{,}486\ \mathrm{C\ mol_{H2O}^{-1}} \times (-1.23\ \mathrm{V}) = 2.37 \times 10^5\ \mathrm{J\ mol_{H2O}^{-1}} > 0$, thus meaning that this process requires energy, which can be provided by a power source moving electrons from the anode to the cathode terminals. As shown in Fig. 1, water is introduced in liquid or vapour form, depending on the temperature, in the anode compartment, where reaction [1] takes place. The protons produced through reaction [1] are transported by the electric field through the PEM to the cathode, where they are reduced according to reaction [2]. The acidic solution is retained in the membrane, thus reducing corrosion problems. The PEM must be thin to reduce the ohmic drop, which allows reducing the voltage needed for the water electrolysis. In addition, it is not an electron conductor and behaves as a separator between the anode and the cathode, thus avoiding internal short-circuits. Moreover, it presents good chemical, mechanical and dimensional stability, with low permeability to H_2 and O_2. The anode and the cathode catalysts layers, CLs in Fig. 1, are placed on each side of the PEM. Over them, the gas diffusion layers (GDLs) allow the diffusion of the reactants. The set integrated by the PEM and the gas and CLs is known as the membrane electrode assembly (MEA). Note also that the reactants circulate through the gas channels of the bipolar plates (BPPs in Fig. 1), which allow building up the complete stack by means of the electrical connection between the cathode and the anode of adjacent cells.

Although PFSAs suffer dehydration over 100 ºC (11) and there is a consequent thermal limit in its practical use, the PEM offers additional advantages to the liquid alkaline electrolyte: (i) there are no anionic concentration gradients (as the anionic charges are fixed, fewer species are transported, and the complexity of the system is reduced); (ii) the gases are evolved at the back of the electrodes and then they do not contribute to the internal cell resistance, which is mainly due to the PEM (5), and (iii) they are free from carbonate formation problems, thus providing highly compressed and pure H_2 with high efficiency (1).

However, unlike the alkaline electrolytes, the acidic ones require corrosion-resistant noble metals as electrocatalysts (12). Main components regarding performance and durability of the PEMWE stacks are the MEAs, in which at present Ir is the electrocatalyst for the OER and Pt for the HER (13)(14)(15)(16). Current densities in the range 0.6-2.0 A cm^{-2} for applied single cell voltages between 1.8-2.2 V can now be obtained (17). PEMWEs are in the early market introduction phase in the energy sector and the focus is on their durability and reliability rather on their cost (13). A recent estimate is that MEAs represent about 19% of the overall stack cost (18). The PEM itself plays a role because it contributes with a significant ohmic loss, increasing with thickness, and must ensure robustness and low H_2 and O_2 crossover. Nafion® 115 and 117, 120-200 μm in thickness are currently used, typically contributing with about 5% of the cost of the PEMWE stack, but there is the possibility to introduce nanoparticles (NPs) or nanofibers in thinner PEMs with lower ionic resistance resulting in good mechanical stability and low O_2 and H_2 crossover (14)(15)(19)(20)(21)(22). The MEA is normally fabricated by depositing directly the

electrocatalysts onto the PEM or by transferring them onto the PEM by a decal process (23). This latter procedure is known as the catalyst coating membrane (CCM) approach (24)(25). The OER presents a more sluggish kinetics than the HER and therefore, it significantly contributes to the overall polarization. Ir metal and IrO_2 are the present state-of-the-art OER catalyst in PEMWEs (12)(14), providing a suitable balance between activity and stability and representing about 8% of the stack cost. With a typical loading of 2 mg_{Ir} cm^{-2} (23), an amount of about 500 kg of Ir is needed for the GW-plant working at 4 W cm^{-2} (14). This is a high amount of Ir when considering the annual worldwide production of about 9,000 kg_{Ir} $year^{-1}$ (2) and therefore, there is the need of reducing the Ir loading while improving the OER performance. The catalyst for the HER is Pt with a loading of about 0.3-0.5 mg cm^{-2} (12)(20)(26), with about 6% of the MEA cost, although it was pointed out that it could be significantly reduced without performance loss (25). Other important components of the PEMWEs are the bipolar plates and the porous transport layers, which contribute with about 68-74% of the overall stack cost (the cell and stack balances account for the remaining %) (14)(18).

PEMWEs use noble metals because of the advantages mentioned above. After intensive research, new components based on non-noble metals may be fruitful in the future (long-term), but in the short-term, there is still room for achieving better performance, durability, and cost reduction with Ir and Pt (14). It is estimated that the overall cost could be reduced to about the half using advanced manufacturing techniques, especially for flow fields and separators (18). The catalytic material and the catalyst loading are also crucial to obtain suitable performance, durability and cost

(14). A good strategy to decrease the catalysts cost can be the use of stable supports enabling a better dispersion to increase their utilization.

Feng et al. (21) have summarized the degradation mechanisms of the components of the PEMWEs. The main concerns of the electrocatalysts were their dissolution, deactivation and agglomeration together with the support passivation (which would impede the current flow), pointing to promising solutions such as addition of inert oxides, the use of binary or ternary solid-solution catalysts or tailoring the morphology of the catalyst. Recent degradation studies of the PEMWEs suggested that the measured cell voltage increase was mainly due to reversible changes in the oxidation state of the Ir-based catalyst, and that the real degradation took place in the ohmic and mass transport overpotential region at high current densities and long-time operation (13).

In this review, the recent approaches to improve performance, stability, durability and cost of the Ir- and Pt-based catalytic materials presently used are examined, as specific objectives in the short-term development of PEMWEs. Thus, main attention has been paid to the catalyst loading and dispersion onto different supports, especially the non-carbonaceous ones, which are particularly important in the anode of the PEMWEs due to the oxidative nature of this environment.

2. Supported Catalysts for the HER

As mentioned in the previous section, the most effective electrocatalysts for the HER in practical PEMWE are those based on Pt. However, the high cost and scarcity of Pt are a drawback in the development of PEMWE large-scale applications. For this

reason, reducing the amount of Pt is the main strategy to decrease the cathode cost contribution to the PEMWEs (25)(28)(29)(30)(31). Pt black has been employed in the cathode of PEMWEs (31), but the Pt loading can be reduced by improving the catalyst dispersion on high specific surface area supports, based on carbon or non-carbon materials. A further strategy involves the development of Pt-based alloys.

2.1. Pt-based catalysts supported on carbon materials

It is generally accepted that highly dispersed Pt-on-C is the benchmark HER catalyst for PEMWEs, the carbon black Vulcan® XC-72 being the most common (15)(19)(22)(23)(25)(26)(27)(30)(32). Carbon-based materials are being widely used as electrocatalyst supports because of their large surface area, high electron conductivity and stability. A PEMWE single cell based on Nafion® NR117 containing 0.4 mg_{Pt} cm^{-2} (40 wt% Pt supported on Vulcan® XC-72) and 2.5 mg cm^{-2} of IrO_2 was reported (32) and it showed 1.7 V at 1 A cm^{-2} and 90 °C. The average degradation rate of voltage was ca. 35.5 µV h^{-1}, after 4000 h at these experimental conditions.

Other materials, like graphitic nanofibers (GNF), have been proposed as catalyst supports because their more suitable textural properties can favour the transport of gases. In particular, the performance obtained with GNF-supported catalysts were found to be better than those obtained with catalysts supported on Vulcan® XC-72 (33). A reduced electrolysis cell voltage (1.67 vs. 1.72 V at 1 A cm^{-2} and 90 °C) was obtained using Pt/GNF cathodes instead of Pt/XC-72 with the same Pt content (40 wt%).

However, the use of carbon supports for stabilizing atomic-scale Pt is challenging because the interaction of the support with Pt atoms must be assured.

Recently, it has been reported in three-electrode cell an ultra-low loading of Pt dispersed on single walled carbon nanotubes, SWNTs (0.19−0.75 at% Pt and a Pt loading of ∼114−570 ng_{Pt} cm^{-2}, respectively), with promising properties in terms of electrocatalytic activity and durability for HER in acidic liquid electrolyte (34). In the same line, more recently, an electrocatalyst comprising Pt nanowires on SWNTs with ultralow Pt content (340 ng_{Pt} cm^{-2}) has been used for the HER (35). A comparable activity (10 mA cm^{-2} at -18 mV vs. RHE) to that of state-of-the-art Pt/C (10 mA cm^{-2} at -16 mV vs. RHE) was reached in acidic aqueous electrolyte. However, it is worth mentioning that HER kinetics cannot be measured accurately in acidic media, because it is limited entirely by H_2 diffusion (36), which requires suitable gas transport techniques (37). In fact, PEMWE single cell tests recorded at 55 °C using Nafion® 115 membrane and 0.02 mg cm^{-2} of Pt/C or Pt/SWNT at the cathode, while having 3 mg cm^{-2} of $IrRuO_x$ at the anode, revealed similar activity. However, the stability of the electrolyser setup operating the cell at the constant current density of 1 A cm^{-2} was better for the MEA containing the Pt/SWNT catalyst.

On the other hand, the H_2 and O_2 permeation between cathode and anode through the membranes of the PEMWEs has been investigated (38)(39)(40) and although O_2 permeation is lower than that of H_2, it increased with current density and temperature (as H_2 permeation did). The O_2 content in the H_2 product was found to be 3-4 times greater when using Pt-free instead of Pt cathode catalysts (39). This was explained by the lower activity for the oxygen reduction using the Pt-free catalyst, so that less permeated O_2 was reduced at the cathode of the PEMWE and consequently, the O_2 flow within H_2 was higher. It has also been reported that permeated O_2 can be

reduced to H_2O_2 at the cathode (two-electron reaction), which can be further transformed into hydroxyl radicals $OH^{\bullet}$ through Fenton's reaction with active metal ion impurities (such as Fe^{2+} and Cu^{2+}) (40). These radicals produce the membrane degradation.

2.2. Pt-based catalysts supported on non-carbon materials

The carbon oxidation of the oxygen cathodes has been reported in polymer electrolyte fuel cells (40) (41) and could also be expected in PEMWEs under given conditions. It is then interesting to explore non-carbonaceous supports with high specific surface area. In this line, TiO_2 has demonstrated very good chemical resistance and thermal stability (42). Shi et al. (43) found that when using a carbon-free Pt/Ti cathode in a PEMWE, the membrane degradation rate was lower when compared to the Pt/C cathode. This was explained by the higher rate of H_2O_2 generation on the carbon surface of the latter, which led to the formation of $OH^{\bullet}$ and $OOH^{\bullet}$ radicals, responsible for the membrane degradation, by reaction with residual active ions such as Fe^{2+}.

Pt NPs supported on nitrogen-doped black TiO_2 (Pt/N_x:TiO_{2-x}) has been reported to show robust durability and onset potentials for the HER, which were somewhat smaller than that of commercial Pt/C catalyst (44). Furthermore, different Pt catalysts supported on Nb-doped TNTs were synthesized and tested for the HER in acidic media (45). Their electrochemical characterization towards HER in acidic aqueous solution showed better performance than those reported in recent literature regarding home-made and commercial Pt supported catalysts. These results make the Pt/Nb-TNT

catalysts, in particular that containing 3 at% Nb, very promising to be applied for the HER in PEMWEs.

2.3. Pt-based alloy catalysts

A further way to reduce the Pt loading in the cathode is by developing active Pt-based alloys. Such would be the case of a recently developed PtFe alloy stabilized with Pt-skin layers supported on carbon black for HER in acidic media (46). The performance and durability of this catalyst was examined in a PEMWE single cell, which incorporated a MEA consisting of Pt_{xAL}–PtFe/C (0.20 mg_{Pt} cm^{-2}) and a conventional anode IrO_2 + Pt black (0.92 mg_{Pt+Ir} cm^{-2}). The electrolyte membrane was commercial Nafion® NRE212 (50 µm thick). The initial cell voltage was 1.57 V at 1.0 A cm^{-2} and 80 °C, and presented an average degradation rate of ~70 µV h^{-1} after 1000 h of continuous operation. This relatively high degradation rate at such rather moderate operating conditions was mainly due to the anode, since the cathode operated with stability with low H_2O_2 production (the cathode potential varied only ~10 mV during this operating time). The challenge in the case of the noble-metal-based bimetallic structures is that they may change during the reaction (47).

There is, of course, an alternative way to decrease the cathode Pt loading. It deals with the MEA manufacture, which would lead to an optimal use of the catalyst and, by extension, the cell performance (25). The PEMWE durability at low catalyst loadings is then the issue. Highly active sites may result from synergistic effects between the supporting materials and the electronic properties of the metal when downsizing to single-atom catalysts, as shown in three-electrode cells (47)(48). However, the undesirably tendency to aggregation remains to be solved.

3. Catalysts for the OER

Even though the electrochemical splitting of water has been known since the 19th century, more knowledge is needed to understand the OER mechanism and to find the ideal catalyst in terms of activity and stability (49). For large-scale production of water electrolysers, the development of highly active, stable, and inexpensive OER catalysts is critical and highly demanded (50).

Due to the sluggish kinetic and the highly oxidative and acidic conditions of the OER, the electrocatalysts used on the anode side have to be noble metals-based, mainly Ir and Ru, because they show the best performance in terms of activity and/or stability in the operation conditions (51)(52)(53). Considering the industrial importance of the PEMWEs, several studies on electrocatalytic properties of Ir- and Ru-based catalysts on OER performance in acidic media are discussed in a large body of literature (27)(49)(52)(53)(54).

Metallic Ru and RuO_2 are known to be the most active catalyst for the OER in acidic media (51)(55)(56). However, several studies have determined the low stability of Ru compared to Ir and other metals, even under mild operation conditions (53)(57)(58). Danilovic et al. (58) used X-ray Absorption Spectroscopy (XAS) together with potentiodynamic OER measurements to establish a functional link between activity and stability of monometallic oxides during the OER in acidic media. They found that the most active oxides (Au $\ll$ Pt < Ir < Ru $\ll$ Os) were, in fact, the least stable (Au $\gg$ Pt > Ir > Ru $\gg$ Os) materials. Discarding Os because of its very low stability, RuO_2 also degrades during OER in acidic media. At potentials higher than 1.4 V, the oxidation of RuO_2 to non-conductive RuO_4 is favoured and tend to dissolve rapidly

(53)(59). Therefore, this reaction greatly modifies RuO_2 properties, significantly losing its electrocatalytic activity and stability during an extended PEMWE operation (52).

A comparative study carried out during OER using an electrochemical scanning flow cell (SFC) connected to an inductively coupled plasma (ICP) mass spectrometer, revealed that IrO_2 was more stable than RuO_2, with a difference in dissolution amounts of ca. 30 times under similar conditions (53). Nowadays, IrO_2 is still outstanding considering both activity and stability and, for this reason, it is used as the state-of-the-art catalyst in PEMWE systems (14)(54).

Unfortunately, the loading of Ir in the anode is significantly higher than the noble metal in the cathode due to the sluggish OER kinetics and stability issue. Moreover, Ir is extremely rare and expensive. For relative small systems (kW range), the Ir and Pt catalysts comprised about 5−10% of the stack cost (60). The catalyst cost is expected to become higher for larger systems (MW range), where the other stack components will be lower (61). Therefore, reducing the loading of precious metals, while maintaining higher activity and optimal stability, is critical to enable large-scale implementation of PEMWEs. For the anode, several strategies are currently pursued, such as reducing the particle size and assuring the uniform distribution over a conductive support to make all nanoparticles electrochemically accessible. When the particle size is reduced (for a given catalyst loading), the effective surface area is increased and thus, more active sites for the OER are formed (62)(63).

3.1. Ir-based core-shell catalysts

In a similar way to Pt, the combination of IrO_2 with other metals in core-shell structures allows using less amount of Ir and, in addition, they could display a superior

OER activity. Tackett et al. (64) described FeN_3 core-IrO_2 shell structures with superior OER activity in which the nitride was protected from the acidic media by the shell and, in addition, the activity increase was related to electronic effects of the substrate-surface interaction. Nong et al. (65) prepared an electrochemically dealloyed IrNi core-IrO_x shell combined with a mesoporous corrosion-resistant Sb-doped SnO_2 support (antimony-tin oxide, ATO), which behaved as highly efficient and stable OER catalysts in acidic medium. The higher OER activity on both geometric surface and Ir-mass basis compared to the IrOx/C and IrOx/commercial ATO benchmarks was explained by electronic and/or strain effects, which could modify the chemisorption and reactivity of intermediates at the surface. More recently, Jiang et al. (66) electrodeposited thin Ir films (~68 nm-thick) on WO_x nanorods, thus allowing a uniform Ir dispersion on the poor conducting WO_x and the use of a low loading of the precious metal. Current densities of 2.2 A cm^{-2} were obtained at 2.0 V in a laboratory PEMWE with a proved stability over 1000 h at 0.5 A cm^{-2} for a reduced loading of 0.14 mg_{Ir} cm^{-2}, which was assigned to the stability of WO_x and the fixing Ir coating.

3.2. Ir-based catalysts with metal oxides

IrO_2 can also be mixed with different metal oxides to lead to electrocatalysts with an improved activity and/or stability for the OER such as $Ru_xIr_{1-x}O_2$ (59), $Ru_{60}Pt_{30}Ir_{10}$ (67), $Ir_{0.7}Ru_{0.3}O_x$ (68)(69)(70) and $Ir_{0.40}Sn_{0.30}Nb_{0.30}O_2$ (71). Computational studies have revealed that the superiority of these mixed metal oxides is due to the stable formation of the intermediates involved in the OER mechanism (72)(73)(74)(75). Tang et al. (76) found that by switching the host structure of the Ir^{4+} oxygen-coordination octahedra from corner- and edge-sharing rutile (IrO_2) to

purely corner-sharing perovskite ($SrIrO_3$), the OER activity increased by more than one order of magnitude. Density functional theory calculations revealed that the adsorption energetics on $SrIrO_3$ depended sensitively on the electron-electron interaction, whereas for IrO_2, it depended rather weakly. On the other hand, Yang et al. (77) reported high-activity face-sharing perovskite structures. Despite the 6H-$SrIrO_3$ perovskite contained 27.1 wt% less Ir than IrO_2, its Ir mass activity was seven times greater than the latter due to the existence of face-sharing IrO_6 octahedral dimers, which facilitated the OER rate determining step by weakening the Ir-O binding.

Another promising solution to decrease the Ir amount is the use of one-dimensional nanoarray electrodes, which shows prominent properties in high utilization of catalyst and enhanced electron and mass transfer (78)(79)(80). Zhao et al. (80) prepared IrOx nanotube arrays by electrodepositing IrO_2 NPs onto ZnO nanorod surfaces to produce IrO_2-coated core–shell nanorod arrays, followed by wet chemical etching the ZnO nano-rods away. The IrO_x nanotube arrays showed 2.7 times higher turnover frequency (TOF) than that of commercial IrO_2 nanoparticle in the OER. Lu et al. (78) prepared vertical aligned IrO_x nanoarrays by electrodeposition using TiO_2 nanotube arrays (TNTA) as template. IrO_x open-end nanotube arrays with tunable length range were obtained by modulating the scan rate in the electrodeposition process. IrO_x nanoarrays performed almost the same OER current density with 1/20 Ir loading amount compared with commercial IrO_2 NPs.

3.3. Ir-based nanostructured thin film catalysts

Other strategy to improve the electrochemical active surface area was the preparation of Ir-based nanostructured thin film (NSTF) electrodes, developed by 3M,

which are less sensitive to agglomeration and corrosion due to the special catalyst morphology (21)(81)(82)(83). The NSTF catalysts were obtained by physical vapor deposition (PVD) of catalysts onto a supported monolayer of oriented crystalline organic-pigment whiskers. Whiskers are corrosion resistant, therefore eliminating the high voltage corrosion affecting most of carbon supports (27). Lewinski et al. (81) prepared an ultra-thin continuous film of Ir deposited on arrays of organic nano-whiskers (PR149). NSTF was shown to be able to operate at 0.25 mg_{Ir}/cm^2 and attain high current densities 10 A/cm^2 @ ~2 V at 80 ºC. More recently, Jensen at al. (83) reported the use of a modified PVD technique for the preparation of interconnected nanoporous thin film by selective leaching of heterogeneous Ir–Co templates prepared by an alternating magnetron sputtering process. This approach allowed the preparation of extended surface area catalysts with higher porosity and Ir dispersion, while maintaining high intrinsic activities. Mirshekari et al. (84) used the reactive spray deposition technology (RSDT), a flame-based process in which the catalyst nanoparticles were synthesized by the combustion of solutions of metal-organic precursors in combustible solvents, to fabricate MEAs with very small amounts of catalysts. Anode and cathode contained only 0.3 mg_{Ir} cm^{-2} (in the form of Ir/IrO_x NPs) and 0.2 mg_{Pt} cm^{-2} (Pt NPs on Vulcan XC-72R), respectively. With the purpose of reducing the H_2 crossover, the MEA contained a thin Pt recombination layer (RL) 100-200 nm in thickness (0.025 mg_{Pt} cm^{-2}) between the Nafion® 211 and the Nafion® 117 membranes of the anode and cathode, also respectively. The cell operated for 3000 h at 50 ºC with 1.8 A cm^{-2} with no significant losses in performance.

3.4. Ir-based catalysts supported on conductive materials

One of the most remarkable ways to achieve highly active electrode with low loading amount of Ir content is the use of conductive supports (67)(85)(86)(87)(88). It has been shown that the supports are important not only to increase the active surface area of the catalysts, but also to integrate the catalyst-support feature in or to improve the charge transfer efficiency between them (89). The stability under the harsh conditions of the cell is one of the main requirements that catalyst supports should meet.

Conductive supports based on carbon materials are routinely used in fuel cell technology. However, under the high potential of the OER, most carbons are easily corroded. Better results were obtained using advanced carbon supports such as carbon nanobowls (90) and nanotubes (91). The stability and activity of Ir nanocrystals supported on carbon nanobowls during the OER at 10 mA cm^{-2} in 0.1 M HClO$_4$ significantly outperformed that of commercial Ir/C (80). IrO$_2$ supported on carbon nanotubes also exhibited similar stability during the OER at the same current density in 0.1 M H$_2$SO$_4$ (88).

3.5. Ir-based catalysts supported on metal oxides

Alternatively, oxide-based supports such as TiO_2 (89)(92)(93)(94), Ti_4O_7 Magneli Phases (70)(95)(96)(97)(98) and doped SnO_2 (60)(85)(87)(99)(100)(101) have been proposed.

3.5.1. TiO_2-based supports

TiO_2 support offers low cost, very high thermal and chemical stability under the anode conditions and commercial availability. However, titania suffers low electric conductivity (about 10^{-6} S cm^{-1} at T < 200 ºC) and low adsorption/desorption capability toward the species and charge in the OER (27)(102)(103)(104). Fuentes et al. (92) developed IrRu(1:1) electrocatalysts supported on anatase TiO_2 with high activity towards the OER, which showed a 53% higher current per gram of metal than that of unsupported electrocatalyst of the same composition. The higher catalyst utilization of the supported electrocatalysts for the OER was consistent with small, well-dispersed nanoparticles. Mazúr et al. (102) prepared IrO_2 NPs (60 wt%) supported on commercial TiO_2 powders, with specific surface areas from 10 to 90 m^2 g^{-1}. They found that the lower the specific surface area of the support the higher was the electrochemical activity of the catalyst. This was explained by the formation of a thin layer of more conductive IrO_2 on the surface of the non-conductive TiO_2, which was able to cover that support with low specific surface area, thus providing the entire material with enough electron conductivity. Rozain et al. (105) synthesized IrO_2 catalysts on micro-sized Ti particles (50 wt% Ti), showing that for IrO_2 loadings less than 0.5 mg$_{IrO2}$ cm^{-2}, the performance of the PEMWE was better than that prepared with unsupported IrO_2. Assuming that Ti was oxidized to TiO_2 during the OER, Bernt

et al. studied the influence of the ionomer content (24) and of the Ir loading (25) on the performance of a PEMWE using IrO_2/TiO_2 (75 wt% Ir) as the anode electrocatalyst. The best performance was found for 11.6 wt% of the ionomer (24). The performance losses below and over this value were ascribed to a higher proton conduction resistance and to an O_2 higher mass transport resistance, respectively. The Ir loading was varied between 0.20–5.41 mg_{Ir} cm^{-2}, the optimal performance at operational current densities ($\geq 1 Acm^{-2}$) being for 1–2 mg_{Ir} cm^{-2}. The CL became very thin and inhomogeneous when its loading was reduced to < 0.5 mgIr cm^{-2}, resulting in a much higher performance loss than expected based simply on the OER kinetics losses (54). This is illustrated in Fig. 2a, where a SEM image of the MEA section is shown. On the anode side, on the left, there is a porous transport layer (PTL) made of sintered Ti, which facilitates the water transport to the CL, composed of IrO_2/TiO_2 and ionomer. Separated by the Nafion® 212 membrane, there is the cathode, made of 4.8 wt% Pt/C and ionomer, covered by a carbon paper PTL. The thickness of the Ir-based CL depends on the Ir load, as shown in Fig. 2b, which shows a couple of examples in the insets. Fig. 3a and b depicts the cross-sectional and top view in the case of a low Ir loading. Fig. 3c and d shows schemes of the electrical connections in the case of thick and thin anode CLs, whereas in Fig. 3e, the Ti PTLs have been replaced by a carbon PTL with a microporous layer (MPL).

Cheng et al. (106) synthesized a composite IrO_x-TiO_2-Ti catalyst with mixed valence Ir species. It was shown that TiO_2 was beneficial for the formation of Ir(III) and mixed Ir(III/IV) oxyhydroxides, resulting in a high surface concentration of adsorbed OH and controllable Ir valence, thus explaining its high OER activity.

Additional durability studies were performed with TiO_2-supported IrO_2 (Elyst Ir75 0480 from Umicore) with an Ir loading of $2mg_{Ir}\,cm^{-2}$ (107). It was observed that the performance of the MEA electrolyser decreased after cycling the anode potential between ~0 V_{RHE} in the open circuit voltage-periods and high potentials when current was applied to the electrolyser. This degradation was due to the formation of the less conductive hydrous $Ir(OH)_x$ phase and the gradual passivation of the titanium porous transport layer (Ti-PTL), which increased the internal ohmic resistance.

The conductivity of TiO_2 could be significantly improved by doping with donor species, such as metal ions. The group of Hong and Lv extensively studied the effect of doping the TiO_2 support for IrO_2 with V (108), Nb (109)(110), Ta (111) and W (112), on the physical properties and OER activity of the catalysts. They obtained highly active IrO_2 supported on mesoporous Nb (20 at%)-doped TiO_2 with specific surface area of $132\,m^2\,g^{-1}$ by means of the modified evaporation-induced self-assembly method (109). The authors found that the majority of the OER activity increase was due to the Nb-doping, which enhanced the specific surface area and surface activity of transferring charge and species. Subsequent treatment of Nb-doped TiO_2 with H_2 resulted in higher electrical conductivity, increased surface active sites and enhanced OER performance (110). The single cell tests showed that the catalyst treated in H_2 at 750 ºC led to the optimum OER activity (1.832 V at 1 $A·cm^{-2}$), which was superior to that of unsupported IrO_2 (1.858 V at 1 $A·cm^{-2}$) and remained stable for 100 h operating at a current density of 1 A cm^{-2}. They also studied the effect of vanadium doping of the TiO_2 support, synthesized by a modified evaporation-induced self-assembly (EISA) technique (113). IrO_2 supported on TiO_2 samples doped with different amounts of V (0, 10, 20, 30 at%)

were evaluated. In single cell, the OER performance gradually increased with V dopant from 0 to 20 at%, followed by a performance deterioration with V amount reaching 30 at% due to the corrodible V_2O_5 precipitate. Recently, the incorporation of W to obtain $IrO_2/Ti_{1-x}W_xO_2$ (x = 0.05, 0.1 and 0.2), resulted in an active electrocatalyst for the OER. Among all the $Ti_{1-x}W_xO_2$ supports, the highest electrocatalytic activity was obtained with $Ti_{0.9}W_{0.1}O_2$. With the optimized IrO_2 loading, the applied potential in a single water electrolysis cell was 1.79 V to obtain 1 A cm^{-2} at 80 °C. The durability tests for $40IrO_2/Ti_{0.9}W_{0.1}O_2$ at 0.5 and 1 A cm^{-2} indicated that the cell voltages were stabilized over 100 h.

Hu et al. (114) synthetized IrO_2 dispersed on a corrosion-resistant $Nb_{0.05}Ti_{0.95}O_2$ support (83 m^{2}g^{-1}) by the sol-gel method. The IrO_2 loading of 26 wt% exhibited the best mass normalized OER activity, which was explained by the uniform supporting of the IrO_2 NPs on the surface, thus providing conductive channels to reduce the grain boundary resistance. Recently, Alcaide et al. (89) prepared IrO_2 and $IrRuO_x$ (50 wt%) supported on titania nanotubes and Nb-doped TiO_2 nanotubes (3 at% Nb). They observed that Nb doping of titania significantly increased the surface area of the support from 145 to 260 m^{2}g^{-1}. The highest OER performance of $IrO_2/Nb-TiO_2$ nanotubes was assigned to the good dispersion and accessibility of the IrO_2 NPs, the high specific surface area of the support and the electron donor properties of the Nb^{4+} species to the conduction band of titania. The stability of the $Nb-TiO_2$ nanotubes was also better than that of unsupported IrO_2.

3.5.2. Ti_nO_{2n-1}-based supports

Non-stoichiometric Ti sub-oxide, TiO_{2-x}, have drawn considerable attention due to their high electronic conductivity. In particular, the Ti sub-oxides Magneli phases, Ti_nO_{2n-1}, such as Ti_5O_9 and Ti_4O_7 or a mixture of them, which are known as the commercial name Ebonex®, are highly conductive and corrosion resistant in acidic media during the OER (95)(115). Metallic Ir NPs supported on Ti_4O_7 was synthetized by Wang et al. (86) via a conventional sodium $NaBH_4$ reduction method in anhydrous ethanol at room temperature. The catalyst exhibited improved OER kinetics in acidic media and higher TOF compared to Ir-black. An study comparing IrO_2 electrocatalysts supported on commercial Ebonex® and Ti-suboxides (Ti_nO_{2n-1}) prepared in-house was carried out by Siracusano et al. (116). The results showed proper electronic conductivity for both electrocatalysts and superior OER activity of the catalyst based on the Ti-suboxides prepared in-house compared to the commercial support. These results were attributed to the better dispersion and larger occurrence of active catalytic sites on the surface of the suboxide prepared in-house.

3.5.3. ATO-based supports

ATO as supporting material has also been considered a good alternative for the OER catalysts because it exhibits relatively high electronic conductivity and corrosion resistance. Some dissolution of the dopant has been reported during the OER at high anodic potentials in H_2SO_4. However, it withstands anodic conditions better than In-doped SnO_2, known as indium-tin oxide, ITO (101). Liu et al. (117) synthetized Sb-SnO_2 nanowires as supporting materials for IrO_2 NPs, which exhibited significant improvement in mass activity when compared to the same catalyst supported on Sb–SnO_2 NPs and pure IrO_2. The OER performance was further confirmed by PEMWE tests

at 80 ºC; the IrO_2/ATO-nw catalyst reached 2 A·cm^{-2} at 1.62 V vs. RHE (80 ºC) with

an activity loss of 0.76 mV·h^{-1} after 646 h at 0.45 A·cm^{-2}. Wang et al. (118) found that

IrO_2 supported on ATO aerogels allowed reducing the use of noble metal while keeping

the same OER current per unit geometric surface area. Furthermore, the highly porous

structure of SnO_2:Sb aerogel was successfully retained by using vanadium additives

under atmospheric drying. However, V did not play any active role in the OER catalysis.

Similarly, Ir NPs supported on SnO_2:Sb aerogel allowed decreasing the use of the

precious metal by more than 70% while enhancing the electrocatalytic activity and

stability (60). Operando near-ambient pressure X-ray photoelectron spectroscopy on

MEAs revealed a low degree of Ir oxidation, attributed to the oxygen spill-over from Ir

to SnO_2:Sb, where the formation of highly unstable Ir^{3+} species was mitigated.

A comprehensive overview about the stability and degradation of catalysts

during the OER in acidic media was given by Spöri et al. (119). They established that

the degree of metal immobilization on the support depends on the interface between

the support surface (groups) and the metal oxide and influences the extent of particle

detachment or dissolution during OER process. These interactions can range from weak

electrostatic attraction to stronger connections through surface chemical bonds or

formation of an overlayer on the support, which can also affect the activity by

decreasing or increasing electron density to the catalyst surface. More recently, several

reviews address the electrocatalysts performance in terms of activity, stability and

efficiency (17)(120)(121). Kim et al. (17) have reviewed the last advances in Ir-based,

Ru-based and even non-noble metal-based multimetallic electrocatalysts for the OER

in acidic media, with emphasis in their stability tests and reference to machine learning

models. Wang et al. (120) have summarized the OER performance of selected catalysts in acidic and alkaline media. Also related to this point, an in-depth literature revision of the OER mechanism, with special emphasis on the adsorption and lattice oxygen evolution mechanisms to elucidate the catalyst degradation, has been recently published by Chen et al. (121).

4. Performance of selected PEMWEs

Table 1 shows the performance of selected PEMWE single cells in the last years, generally at 80 °C, including catalyst loading, operating conditions, type of membrane and degradation rate, which have been discussed along this paper. Along this review, we have seen many different anodic and cathodic catalysts, which have been studied in three-electrode cells and/or in laboratory PEMWEs. Note that the latter have been generally tested using Pt supported on carbon cathodes and different PEMs, also applying different voltages (resulting in different current densities). It is not then easy to extract the best PEMWEs, since changing the anode, the cathode, the membrane, the temperature, the cell voltage and/or catalysts loadings can lead to significant changes in the cell performance. An optimization of all these parameters should be performed. However, promising results can be ascertained. General trends can be observed through the last years: i) Current densities and cell voltages are similar, but the most recent papers use less amount of Ir at the anode due to a better dispersion of the precious metal (on a supporting material or unsupported, although obtained using a different synthesis procedure); ii) A gain in the PEMWE stability is also appreciated (between the several factors affecting the PEMWE stability, there is the anode structure and the membrane degradation); iii) Efforts in limiting the permeation of gases through the membrane led to a better PEMWE stability (radicals formed at the cathode produce the membrane degradation).

5. Concluding remarks

In this review, an overview on the most recent advances in electrocatalysis for PEM water electrolysis have been provided, both for the HER at the cathode and the OER at the anode, paying special attention to the development of noble metal supported catalysts and their implementation into practical systems. For the former reaction, Pt/C is the most common catalyst, while for the latter the most used catalysts are Ir black and IrO_2. Both noble metals are scarce and expensive. In this sense, several approaches to develop highly structured catalysts leading to high metal dispersion and, ultimately, lower loadings at the electrodes, have been thoroughly reviewed. Regarding HER, Pt supported on advanced carbon materials provides the solution to achieve the expected targets in terms of performance, but in the authors' opinion, durability is an issue that requires the use of alternative Ti-based non-carbon supports. Regarding the OER, among the reviewed approaches and also in the authors' opinion, the development of Ir-based catalysts supported on conductive metal oxides such as those based on Nb-doped TiO_2 and Sb-doped SnO_2 could lead to the expected performance and durability required by the industry players.

Overall, in the short term, the development of advanced supports for metal dispersion will allow optimizing the use of these noble metals, reducing the cost, and increasing the performance and durability of the electrolysers. In the long term, the development of non-noble catalysts and their implementation in real cells is mandatory to ensure the viability of the technology. In this sense, preliminary studies carried out with non-noble catalysts in half-cell configuration are promising, but further work is necessary to improve their stability and durability in practical cells. Thus, there is still a long way to go before their implementation in commercial PEMWEs.

REFERENCES

1. K. Bareiß, C. de la Rua, M. Möckl and T. Hamacher, *Appl. Energy*, 2019, **237**, 862 LINK https://doi.org/10.1016/j.apenergy.2019.01.001

2. P. C. K. Vesborg and T. F. Jaramillo, *RSC Adv.*, 2012, **2**, (21), 7933 LINK https://doi.org/10.1039/C2RA20839C

3. M. Pudukudy, Z. Yaakob, M. Mohammad, B. Narayanan and K. Sopian, *Renew. Sustain. Energy Rev.*, 2014, **30**, 743 LINK https://doi.org/10.1016/j.rser.2013.11.015

4. P. Nikolaidis and A. Poullikkas, *Renew. Sustain. Energy Rev.*, 2017, **67**, 597 LINK https://doi.org/10.1016/j.rser.2016.09.044

5. Y. Naimi and A. Antar, 'Hydrogen Generation by Water Electrolysis', in 'Advances in Hydrogen Generation Technologies', InTechOpen, 2018, Chap. 1 LINK https://doi.org/10.5772/intechopen.76814

6. D. M. F. Santos, C. A. C. Sequeira, J. L. Figueiredo, Quim. Nova, 2013, 36, (8), 1176 LINK http://dx.doi.org/10.1590/S0100-40422013000800017

7. D. Berndt, D. Spahrbier, in Ullmann's Encyclopedia of Industrial Chemistry, Wiley-VCH: Weinheim, 2005

8. J. Brauns, T. Turek, Processes, 2020, 8, 248 LINK https://doi.org/10.3390/pr8020248

9. A. S. Aricò, S. Siracusano, N. Briguglio, V. Baglio, A. Di Blasi and V. Antonucci, *J. Appl. Electrochem.*, 2013, **43**, (2), 107 LINK https://doi.org/10.1007/s10800-012-0490-5

10. X. Sun, K. Xu, C. Fleischer, X. Liu, M. Grandcolas, R. Strandbakke, T. S. Bjørheim,

T. Norby and A. Chatzitakis, *Catalysts*, 2018, **8**, 657 LINK https://doi.org/10.3390/catal8120657

11. A. Kusoglu and A. Z. Weber, *Chem. Rev.*, 2017, **117**, 987 LINK https://doi.org/10.1021/acs.chemrev.6b00159

12. P. Millet, N. Mbemba, S. A. Grigoriev, V. N. Fateev, A. Aukauloo and C. Etiévant, *Int. J. Hydrogen Energy*, 2011, **36**, (6), 4134 LINK https://doi.org/10.1016/j.ijhydene.2010.06.105

13. M. Suermann, B. Bensmann and R. Hanke-Rauschenbach, *J. Electrochem. Soc.*, 2019, **166**, (10), F645 LINK https://doi.org/10.1149/2.1451910jes

14. P. Shirvanian and F. van Berkel, *Electrochem. Commun.*, 2020, **114**, 106704 LINK https://doi.org/10.1016/j.elecom.2020.106704

15. P. Holzapfel, M. Bühler, C. Van Pham, F. Hegge, T. Böhm, D. McLaughlin, M. Breitwieser and S. Thiele, *Electrochem. commun.*, 2020, **110**, LINK https://doi.org/10.1016/j.elecom.2019.106640

16. T. Reier, M. Oezaslan and P. Strasser, *ACS Catal.*, 2012, **2**, 1765 LINK https://dx.doi.org/10.1021/cs3003098

17. T. Kim, B. Kim, T. Kwon, H. Y. Kim, J. Y. Kim and K. Lee, *Mater. Chem. Front.*, 2021 LINK https://doi.org/10.1039/d1qm00138h

18. K. Ayers, N. Danilovic, R. Ouimet, M. Carmo, B. Pivovar and M. Bornstein, *Annu. Rev. Chem. Biomol. Eng.*, 2019, **10**, 219 LINK https://doi.org/10.1146/annurev-chembioeng-060718-030241

19. C. Klose, P. Trinke, T. Böhm, B. Bensmann, S. Vierrath, R. Hanke-Rauschenbach and S. Thiele, *J. Electrochem. Soc.*, 2018, **165**, (16), F1271 LINK

https://doi.org/10.1149/2.1241814jes

20. J. Hu, J. Luo, P. Wagner, O. Conrad and C. Agert, *Electrochem. commun.*, 2009, **11**, (12), 2324 LINK https://doi.org/10.1016/j.elecom.2009.10.020

21. Q. Feng, X. Z. Yuan, G. Liu, B. Wei, Z. Zhang, H. Li and H. Wang, *J. Power Sources*, 2017, **366**, 33 LINK https://doi.org/10.1016/j.jpowsour.2017.09.006

22. M. Bühler, F. Hegge, P. Holzapfel, M. Bierling, M. Suermann, S. Vierrath and S. Thiele, *J. Mater. Chem. A*, 2019, **7**, (47), 26984 LINK https://doi.org/10.1039/c9ta08396k

23. M. Stähler, A. Stähler, F. Scheepers, M. Carmo and D. Stolten, *Int. J. Hydrogen Energy*, 2019, **44**, (14), 7053 LINK https://doi.org/10.1016/j.ijhydene.2019.02.016

24. M. Bernt and H. A. Gasteiger, *J. Electrochem. Soc.*, 2016, **163**, (11), F3179 LINK https://doi.org/10.1149/2.0231611jes

25. M. Bernt, A. Siebel and H. A. Gasteiger, *J. Electrochem. Soc.*, 2018, **165**, (5), F305 LINK https://doi.org/10.1149/2.0641805jes

26. M. Stähler, A. Stähler, F. Scheepers, M. Carmo, W. Lehnert and D. Stolten, *Int. J. Hydrogen Energy*, 2020, **45**, (7), 4008 LINK https://doi.org/10.1016/j.ijhydene.2019.12.016

27. M. Carmo, D. L. Fritz, J. Mergel and D. Stolten, *Int. J. Hydrogen Energy*, 2013, **38**, (12), 4901 LINK https://dx.doi.org/10.1016/j.ijhydene.2013.01.151

28. M. Bajdich, M. García-Mota, A. Vojvodic, J. K. Nørskov and A. T. Bell, *J. Am. Chem. Soc.*, 2013, **135**, (36), 13521 LINK https://doi.org/10.1021/ja405997s

29. S. Shiva Kumar and V. Himabindu, *Mater. Sci. Energy Technol.*, 2019, **2**, (3), 442

LINK https://doi.org/10.1016/j.mset.2019.03.002

30. S. Shiva Kumar and V. Himabindu, *Renew. Energy*, 2020, **146**, 2281 LINK https://doi.org/10.1016/j.renene.2019.08.068

31. Z. Kang, G. Yang, J. Mo, Y. Li, S. Yu, D. A. Cullen, S. T. Retterer, T. J. Toops, G. Bender, B. S. Pivovar, J. B. Green and F. Y. Zhang, *Nano Energy*, 2018, **47**, 434 LINK https://doi.org/10.1016/j.nanoen.2018.03.015

32. S. A. Grigoriev and A. A. Kalinnikov, *Int. J. Hydrogen Energy*, 2017, **42**, (3), 1590 LINK https://doi.org/10.1016/j.ijhydene.2016.09.058

33. S. A. Grigoriev, M. S. Mamat, K. A. Dzhus, G. S. Walker, P. Millet, *Int. J. Hydrogen Energy*, 2011, **36**, 4143 LINK: doi:10.1016/j.ijhydene.2010.07.013

34. M. Tavakkoli, N. Holmberg, R. Kronberg, H. Jiang, J. Sainio, E. I. Kauppinen, T. Kallio and K. Laasonen, *ACS Catal.*, 2017, **7**, (5), 3121 LINK https://doi.org/10.1021/acscatal.7b00199

35. T. Rajala, R. Kronberg, R. Backhouse, M. E. M. Buan, M. Tripathi, A. Zitolo, H. Jiang, K. Laasonen, T. Susi, F. Jaouen and T. Kallio, *Appl. Catal. B Environ.*, 2020, **265**, LINK https://doi.org/10.1016/j.apcatb.2019.118582

36. W. Sheng, H. A. Gasteiger, Y. Shao-Horn, *J. Electrochem. Soc.*, 2010, **157**, B1529 LINK: https://doi.org/10.1149/1.3483106

37. C. M. Zalitis, D. Kramer, A. R. Kucernak, *Phys. Chem. Chem. Phys.*, 2013, **15**, 4329 LINK: https://doi.org/10.1039/C3CP44431G

38. E. Price, *Johnson Matthey Technol. Rev.*, 2017, **61**, (1), 47 LINK https://doi.org/10.1595/205651317X693732

39. P. Trinke, B. Bensmann and R. Hanke-Rauschenbach, *Electrochem. commun.*,

2017, **82**, 98 LINK https://doi.org/10.1016/j.elecom.2017.07.018

40. M. Chandesris, V. Médeau, N. Guillet, S. Chelghoum, D. Thoby and F. Fouda-Onana, *Int. J. Hydrogen Energy*, 2015, **40**, (3), 1353 LINK https://doi.org/10.1016/j.ijhydene.2014.11.111

41. A. A. Franco and M. Gerard, *J. Electrochem. Soc.*, 2008, **155**, (4), B367 LINK http://dx.doi.org/10.1149/1.2838165

42. X. Chen and S. S. Mao, *Chem. Rev.*, 2007, **107**, (7), 2891 LINK https://doi.org/10.1021/cr0500535

43. Y. Shi, L. Guo, Z. Lu, Z. Wang, Y. Gan, C. Guo, H. Tan and C. Yan, Energy Technol., 2019, 7, 1800781 LINK https://doi.org/10.1002/ente.201800781

44. X. Wang, X. Yuan, X. Liu, W. Dong, C. Dong, M. Lou, J. Li, T. Lin and F. Huang, *J. Alloys Compd.*, 2017, **701**, 669 LINK https://doi.org/10.1016/j.jallcom.2017.01.152

45. F. Alcaide, R. V. Genova, G. Álvarez, H. J. Grande, Ó. Miguel and P. L. Cabot, *Int. J. Hydrogen Energy*, 2020, LINK https://doi.org/10.1016/j.ijhydene.2020.01.057

46. G. Shi, H. Yano, D. A. Tryk, S. Nohara and H. Uchida, *Phys. Chem. Chem. Phys.*, 2019, **21**, (6), 2861 LINK https://doi.org/10.1039/C8CP06825A

47. C. Li, J.-B. Baek, *ACS Omega*, 2020, **5**, 31 LINK https://doi.org/10.1021/acsomega.9b03550

48. N. Cheng, S. Stambula, D. Wang, M. N. Banis, J. Liu, A. Riese, B. Xiao, R. Li, T.-K. Sham, L.-M. Liu, G. A. Botton, X. Sun, *Nat. Commun.*, 2016, **7**, 13638 LINK https://doi.org/10.1038/ncomms13638

49. E. Fabbri and T. J. Schmidt, *ACS Catal.*, 2018, **8**, (10), 9765 LINK

https://doi.org/10.1021/acscatal.8b02712

50. N.-T. Suen, S.-F. Hung, Q. Quan, N. Zhang, Y.-J. Xu and H. M. Chen, *Chem. Soc. Rev.*, 2017, **46**, (2), 337 LINK https://doi.org/10.1039/C6CS00328A

51. S. Trasatti, *Electrochim. Acta*, 1984, **29**, (11), 1503 LINK https://doi.org/10.1016/0013-4686(84)85004-5

52. S. Park, Y. Shao, J. Liu and Y. Wang, *Energy Environ.Sci.*, 2012, **5**, 9331

53. S. Cherevko, S. Geiger, O. Kasian, N. Kulyk, J.-P. Grote, A. Savan, B. R. Shrestha, S. Merzlikin, B. Breitbach, A. Ludwig and K. J. J. Mayrhofer, *Catal. Today*, 2016, **262**, 170 LINK https://doi.org/https://doi.org/10.1016/j.cattod.2015.08.014

54. M. Bernt, A. Hartig-Weiß, M. F. Tovini, H. A. El-Sayed, C. Schramm, J. Schröter, C. Gebauer and H. A. Gasteiger, *Chem. Ing. Tech.*, 2020, **92**, 31 LINK https://doi.org/10.1002/cite.201900101

55. C. Iwakura, K. Hirao and H. Tamura, *Electrochim. Acta*, 1977, **22**, (4), 329 LINK https://doi.org/10.1016/0013-4686(77)85082-2

56. E. A. Paoli, F. Masini, R. Frydendal, D. Deiana, C. Schlaup, M. Malizia, T. W. Hansen, S. Horch, I. E. L. Stephens and I. Chorkendorff, *Chem. Sci.*, 2015, **6**, (1), 190 LINK https://doi.org/10.1039/c4sc02685c

57. M. Escudero-Escribano, A. F. Pedersen, E. A. Paoli, R. Frydendal, D. Friebel, P. Malacrida, J. Rossmeisl, I. E. L. Stephens and I. Chorkendorff, *J. Phys. Chem. B*, 2018, **122**, (2), 947 LINK https://doi.org/10.1021/acs.jpcb.7b07047

58. N. Danilovic, R. Subbaraman, K.-C. Chang, S. H. Chang, Y. Kang, J. D. Snyder, A. P. Paulikas, D. Strmcnik, Y.-T. Kim, D. J. Myers, V. R. Stamenkovic and N. M. Markovic, *J. Phys. Chem. Lett.*, 2014, LINK https://doi.org/10.1021/jz501061n

59. R. Kötz and S. Stucki, *Electrochim. Acta*, 1986, **31**, (10), 1311 LINK https://doi.org/http://dx.doi.org/10.1016/0013-4686(86)80153-0

60. V. A. Saveleva, L. Wang, O. Kasian, M. Batuk, J. Hadermann, J. J. Gallet, F. Bournel, N. Alonso-Vante, G. Ozouf, C. Beauger, K. J. J. Mayrhofer, S. Cherevko, A. S. Gago, K. A. Friedrich, S. Zafeiratos and E. R. Savinova, *ACS Catal.*, 2020, **10**, (4), 2508 LINK https://doi.org/10.1021/acscatal.9b04449

61. K. E. Ayers, J. N. Renner, N. Danilovic, J. X. Wang, Y. Zhang, R. Maric and H. Yu, *Catal. Today*, 2016, **262**, 121 LINK https://doi.org/10.1016/j.cattod.2015.10.019

62. X. Xia, L. Figueroa-Cosme, J. Tao, H. C. Peng, G. Niu, Y. Zhu and Y. Xia, *J. Am. Chem. Soc.*, 2014, **136**, (31), 10878 LINK https://doi.org/10.1021/ja505716v

63. S. Siracusano, V. Baglio, S. A. Grigoriev, L. Merlo, V. N. Fateev and A. S. Aricò, *J. Power Sources*, 2017, **366**, 105 LINK https://doi.org/10.1016/j.jpowsour.2017.09.020

64. B. M. Tackett, W. Sheng, S. Kattel, S. Yao, B. Yan, K. A. Kuttiyiel, Q. Wu and J. G. Chen, *ACS Catal.*, 2018, **8**, (3), 2615 LINK https://doi.org/10.1021/acscatal.7b04410

65. H. N. Nong, H. S. Oh, T. Reier, E. Willinger, M. G. Willinger, V. Petkov, D. Teschner and P. Strasser, *Angew. Chem. Int. Ed.*, 2015, **54**, (10), 2975 LINK https://doi.org/10.1002/anie.201411072

66. G. Jiang, H. Yu, Y. Li, D. Yao, J. Chi, S. Sun and Z. Shao, *ACS Appl. Mater. Interfaces,* 2021, **13**, 15073 LINK https://doi.org/10.1021/acsami.0c20791

67. K. C. Neyerlin, G. Bugosh, R. Forgie, Z. Liu and P. Strasser, *J. Electrochem. Soc.*,

2009, **156**, (3), B363 LINK https://doi.org/10.1149/1.3049820

68. S. Siracusano, N. Van Dijk, E. Payne-Johnson, V. Baglio and A. S. Aricò, *Appl. Catal. B Environ.*, 2015, **164**, 488 LINK https://doi.org/10.1016/j.apcatb.2014.09.005

69. S. Siracusano, S. Trocino, N. Briguglio, F. Pantò and A. S. Aricò, *J. Power Sources*, 2020, **468**, LINK https://doi.org/10.1016/j.jpowsour.2020.228390

70. L. Wang, V. A. Saveleva, S. Zafeiratos, E. R. Savinova, P. Lettenmeier, P. Gazdzicki, A. S. Gago and K. A. Friedrich, *Nano Energy*, 2017, **34**, 385 LINK https://doi.org/10.1016/j.nanoen.2017.02.045

71. K. Kadakia, M. K. Datta, O. I. Velikokhatnyi, P. Jampani, S. K. Park, P. Saha, J. A. Poston, A. Manivannan and P. N. Kumta, *Int. J. Hydrogen Energy*, 2012, **37**, (4), 3001 LINK https://doi.org/10.1016/j.ijhydene.2011.11.055

72. I. C. Man, H. Y. Su, F. Calle-Vallejo, H. A. Hansen, J. I. Martínez, N. G. Inoglu, J. Kitchin, T. F. Jaramillo, J. K. Nørskov and J. Rossmeisl, *ChemCatChem*, 2011, **3**, (7), 1159

73. A. Eftekhari, *Mater. Today Energy*, 2017, **5**, 37 LINK https://doi.org/10.1016/j.mtener.2017.05.002

74. J. Rossmeisl, Z. W. Qu, H. Zhu, G. J. Kroes and J. K. N+©rskov, *J. Electroanal. Chem.*, 2007, **607**, (1GÇô2), 83

75. M. T. M. Koper, *J. Electroanal. Chem.*, 2011, **660**, (2), 254 LINK https://doi.org/10.1016/j.jelechem.2010.10.004

76. R. Tang, Y. Nie, J. K. Kawasaki, D. Y. Kuo, G. Petretto, G. Hautier, G. M. Rignanese, K. M. Shen, D. G. Schlom and J. Suntivich, *J. Mater. Chem. A*, 2016, **4**, (18),

6831 LINK https://doi.org/10.1039/c5ta09530a

77. L. Yang, G. Yu, X. Ai, W. Yan, H. Duan, W. Chen, X. Li, T. Wang, C. Zhang, X. Huang, J. S. Chen, X. Zou, *Nat. Commun.*, 2018, **9**, 5236 LINK https://doi.org/10.1038/s41467-018-07678-w

78. Z. X. Lu, Y. Shi, P. Gupta, X. ping Min, H. yi Tan, Z. Da Wang, C. qing Guo, Z. qing Zou, H. Yang, S. Mukerjee and C. F. Yan, *Electrochim. Acta*, 2020, **348**, LINK https://doi.org/10.1016/j.electacta.2020.136302

79. Q. Shi, C. Zhu, D. Du, J. Wang, H. Xia, M. H. Engelhard, S. Feng and Y. Lin, *J. Mater. Chem. A*, 2018, **6**, (19), 8855 LINK https://doi.org/10.1039/c8ta01288a

80. C. Zhao, H. Yu, Y. Li, X. Li, L. Ding and L. Fan, *J. Electroanal. Chem.*, 2013, **688**, 269 LINK https://doi.org/10.1016/j.jelechem.2012.08.032

81. K. A. Lewinski, D. van der Vliet and S. M. Luopa, *ECS Trans.*, 2015, **69**, (17), 893 LINK https://doi.org/10.1149/06917.0893ecst

82. R. T. Atanasoski, L. L. Atanasoska, D. A. Cullen, G. M. Haugen, K. L. More and G. D. Vernstrom, *Electrocatalysis*, 2012, **3**, (3), 284 LINK https://doi.org/10.1007/s12678-012-0092-3

83. A. W. Jensen, G. W. Sievers, K. D. Jensen, J. Quinson, A. Arminio-ravelo, V. Brüser, M. Arenz and M. Escudero-Escribano, *J. Mater. Chem. A*, 2020, **8**, 1066 LINK https://doi.org/10.1039/c9ta12796h

84. G. Mirshekari, R. *Ouimet*, Z. Zeng, H. Yu, S. Bliznakov, L. Bonville, A. Niedzwiecki, C. Capuano, K. Ayers and R. Maric, *Int. J. Hydrogen Energy*, 2021, **46**, 1526 LINK https://doi.org/10.1016/j.ijhydene.2020.10.112

85. H. S. Oh, H. N. Nong, T. Reier, M. Gliech and P. Strasser, *Chem. Sci.*, 2015, **6**,

(6), 3321 LINK https://doi.org/10.1039/c5sc00518c

86. L. Wang, P. Lettenmeier, U. Golla-Schindler, P. Gazdzicki, N. A. Cañas, T. Morawietz, R. Hiesgen, S. S. Hosseiny, A. S. Gago and K. A. Friedrich, *Phys. Chem. Chem. Phys.*, 2016, **18**, (6), 4487 LINK https://doi.org/10.1039/c5cp05296c

87. L. Solà-Hernández, F. Claudel, F. Maillard and C. Beauger, *Int. J. Hydrogen Energy*, 2019, **44**, (45), 24331 LINK https://doi.org/10.1016/j.ijhydene.2019.07.152

88. A. B. Jorge, I. Dedigama, T. S. Miller, P. Shearing, D. J. L. Brett and P. F. McMillan, *Nanomaterials*, 2018, **8**, (6), LINK https://doi.org/10.3390/nano8060432

89. R. V Genova-Koleva, F. Alcaide, G. Álvarez, P. L. Cabot, H.-J. Grande, M. V Martínez-Huerta and O. Miguel, *J. Energy Chem.*, 2019, LINK https://doi.org/https://doi.org/10.1016/j.jechem.2019.03.008

90. Q. Xue, W. Gao, J. Zhu, R. Peng, Q. Xu, P. Chen and Y. Chen, *J. Colloid Interface Sci.*, 2018, **529**, 325 LINK https://doi.org/10.1016/j.jcis.2018.06.014

91. R. Badam, M. Hara, H. H. Huang and M. Yoshimura, *Int. J. Hydrogen Energy*, 2018, **43**, (39), 18095 LINK https://doi.org/10.1016/j.ijhydene.2018.08.034

92. R. E. Fuentes, J. Farell and J. W. Weidner, *Electrochem. Solid-State Lett.*, 2011, **14**, (3), E5

93. M. Garcia-Mota, A. Vojvodic, H. Metiu, I. C. Man, H. Y. Su, J. Rossmeisl and J. K. N+©rskov, *ChemCatChem*, 2011, **3**, (10), 1607

94. M. Aizawa, S. Lee and S. L. Anderson, *Surf. Sci.*, 2003, **542**, (3), 253 LINK https://doi.org/10.1016/S0039-6028(03)00984-1

95. F. C. Walsh and R. G. A. Wills, *Electrochim. Acta*, 2010, **55**, (22), 6342 LINK

https://doi.org/10.1016/j.electacta.2010.05.011

96. S.-S. Huang, Y.-H. Lin, W. Chuang, P.-S. Shao, C.-H. Chuang, J.-F. Lee, M.-L. Lu, Y.-T. Weng and N.-L. Wu, *ACS Sustain. Chem. Eng.*, 2018, **6**, (3), 3162 LINK https://doi.org/10.1021/acssuschemeng.7b03189

97. K. Huang, Y. Li and Y. Xing, *J. Mater. Res.*, 2013, **28**, (3), 454 LINK https://doi.org/10.1557/jmr.2012.353

98. A. Kitada, G. Hasegawa, Y. Kobayashi, K. Kanamori, K. Nakanishi and H. Kageyama, *J. Am. Chem. Soc.*, 2012, **134**, (26), 10894 LINK https://doi.org/10.1021/ja302083n

99. M. P. Gurrola, J. Gutiérrez, S. Rivas, M. Guerra-Balcázar, J. Ledesma-García and L. G. Arriaga, Int. J. Hydrogen Energy, 2014, **39**, 16763 LINK https://doi.org/10.1016/j.ijhydene.2014.02.156

100. S. B. Han, Y. H. Mo, Y. S. Lee, S. G. Lee, D. H. Park and K. W. Park, *Int. J. Hydrogen Energy*, 2020, **45**, 1409 LINK https://doi.org/10.1016/j.ijhydene.2019.11.109

101. S. Geiger, O. Kasian, A. M. Mingers, K. J. J. Mayrhofer and S. Cherevko, *Sci. Rep.*, 2017, **7**, 4595 LINK https://doi.org/10.1038/s41598-017-04079-9

102. P. Mazúr, J. Polonský, M. Paidar and K. Bouzek, *Int. J. Hydrogen Energy*, 2012, **37**, 12081 LINK https://doi.org/10.1016/j.ijhydene.2012.05.129

103. Y. C. Nah, I. Paramasivam and P. Schmuki, 'Doped TiO2 and TiO2 Nanotubes: Synthesis and Applications', 'ChemPhysChem', Wiley-VCH Verlag, 2010 LINK https://doi.org/10.1002/cphc.201000276

104. G. Garcia-Belmonte, V. Kytin, T. Dittrlch and J. Bisquert, *J. Appl. Phys.*, 2003,

94, (8), 5261 LINK https://doi.org/10.1063/1.1610805

105. C. Rozain, E. Mayousse, N. Guillet and P. Millet, *Appl. Catal. B Environ.*, 2016, **182**, 123 LINK http://dx.doi.org/10.1016/j.apcatb.2015.09.011

106. J. Cheng, J. Yang, S. Kitano, G. Juhasz, M. Higashi, M. Sadakiyo, K. Kato, S. Yoshioka, T. Sugiyama, M. Yamauchi and N. Nakashima, *ACS Catal.*, 2019, **9**, 6974 LINK https://doi.org/10.1021/acscatal.9b01438

107. A. Weiß, A. Siebel, M. Bernt, T.-H. Shen, V. Tileli and H. A. Gasteiger, *J. Electrochem. Soc.*, 2019, **166**, (8), F487 LINK https://doi.org/10.1149/2.0421908jes

108. C. Hao, H. Lv, Q. Zhao, B. Li, C. Zhang, C. Mi, Y. Song and J. Ma, *Int. J. Hydrogen Energy*, 2017, **42**, (15), 9384 LINK https://doi.org/10.1016/j.ijhydene.2017.02.131

109. C. Hao, H. Lv, C. Mi, Y. Song and J. Ma, *ACS Sustain. Chem. Eng.*, 2016, **4**, (3), 746 LINK https://doi.org/10.1021/acssuschemeng.5b00531

110. H. Lv, S. Wang, C. Hao, W. Zhou, J. Li, M. Xue and C. Zhang, *ChemCatChem*, 2019, **11**, (10), 2511 LINK https://doi.org/10.1002/cctc.201900090

111. H. Lv, G. Zhang, C. Hao, C. Mi, W. Zhou, D. Yang, B. Li and C. Zhang, *RSC Adv.*, 2017, **7**, (64), 40427 LINK https://doi.org/10.1039/c7ra06534e

112. H. Lv, J. Zuo, W. Zhou, X. Shen, B. Li, D. Yang, Y. Liu, L. Jin and C. Zhang, *J. Electroanal. Chem.*, 2019, **833**, 471 LINK https://doi.org/10.1016/j.jelechem.2018.12.008

113. C. Hao, H. Lv, Q. Zhao, B. Li, C. Zhang, C. Mi, Y. Song and J. Ma, *Int. J. Hydrogen Energy*, 2017, **42**, (15), 9384 LINK

https://doi.org/10.1016/j.ijhydene.2017.02.131

114. W. Hu, S. Chen and Q. Xia, *Int. J. Hydrogen Energy*, 2014, **39**, (13), 6967 LINK
https://doi.org/10.1016/j.ijhydene.2014.02.114

115. S. S. Huang, Y. H. Lin, W. Chuang, P. S. Shao, C. H. Chuang, J. F. Lee, M. L. Lu,
Y. T. Weng and N. L. Wu, *ACS Sustain. Chem. Eng.*, 2018, **6**, (3), 3162 LINK
https://doi.org/10.1021/acssuschemeng.7b03189

116. S. Siracusano, V. Baglio, C. D'Urso, V. Antonucci and A. S. Aricò, *Electrochim.
Acta*, 2009, **54**, (26), 6292 LINK
https://doi.org/10.1016/j.electacta.2009.05.094

117. G. Liu, J. Xu, Y. Wang and X. Wang, *J. Mater. Chem. A*, 2015, **3**, (41), 20791
LINK https://doi.org/10.1039/c5ta02942b

118. L. Wang, F. Song, G. Ozouf, D. Geiger, T. Morawietz, M. Handl, P. Gazdzicki, C.
Beauger, U. Kaiser, R. Hiesgen, A. S. Gago and K. A. Friedrich, *J. Mater. Chem.
A*, 2017, **5**, (7), 3172 LINK https://doi.org/10.1039/c7ta00679a

119. C. Spöri, J. T. H. Kwan, A. Bonakdarpour, D. P. Wilkinson and P. Strasser, *Angew.
Chem. Int. Ed.*, 2017, **56**, 5994 LINK https://doi.org/10.1002/anie.201608601

120. S. Wang, A. Lu and C.-J. Zhong, *Nano Convergence*, 2021, 8:4 LINK
https://doi.org/10.1186/s40580-021-00254-x

121. Z. Chen, L. Guo, L. Pan, T. Yan, Z. He, Y. Li, C. Shi, Z.-F. Huang, X. Zhang and
J.-J. Zou, *Adv. Energy Mater.*, 2022, **12**, 2103670 LINK
https://doi.org/10.1002/aenm.202103670

The Authors

Dr. Pere L. Cabot defended his PhD in 1984 at the *Universitat de Barcelona* (UB) and is Full Professor of the Department of Materials Science and Physical Chemistry (Section of Physical Chemistry) of the UB since 2003. His current research is Electrocatalysis in Fuel Cell and Electrolyzers, with special interest in polymetallic nanostructures and catalysts supports. He has participated in 50 competitive research projects, 31 contracts with companies and published 170 research papers, 3 international patents, 23 books and book chapters and about 200 meeting presentations and invited lectures. He has also received 3 awards from private companies, related to research, development and innovation.

Dr. Maria Victoria Martínez Huerta holds a Tenured Scientist position at the Institute of Catalysis and Petrochemistry (ICP) of the Spanish Council for Scientific Research (CSIC) from 2010, and is the head of the Electrocatalysis for Energy and the Environment Group. Her research activity is dedicated to the development of electrocatalysts that improve the activity and stability of electrodes in electrochemical devices for storage and conversion of clean energy, mainly in those applications that use hydrogen as an energy carrier such as fuel cells and electrolysers. She has participated in 39 competitive research projects and published 89 research papers (ISI).

Dr. Francisco Alcaide Monterrubio holds a PhD in Chemistry (Physical Chemistry) by the University of Barcelona (2002). He has more than 25 years of experience in electrochemical technologies, specially, in fuel cells & hydrogen. He has participated, and led, in about 50 R+D+I national, European, and international projects and contracts with companies, and in technology transfer and innovation. He serves as independent expert and advisor for several national, international and EC public bodies. His research interests range from electrodics and electrocatalysis for clean energy and decarbonisation to batteries and water treatment. Dr. Alcaide currently works as Principal Investigator and Project manager at CIDETEC.

<Figures>
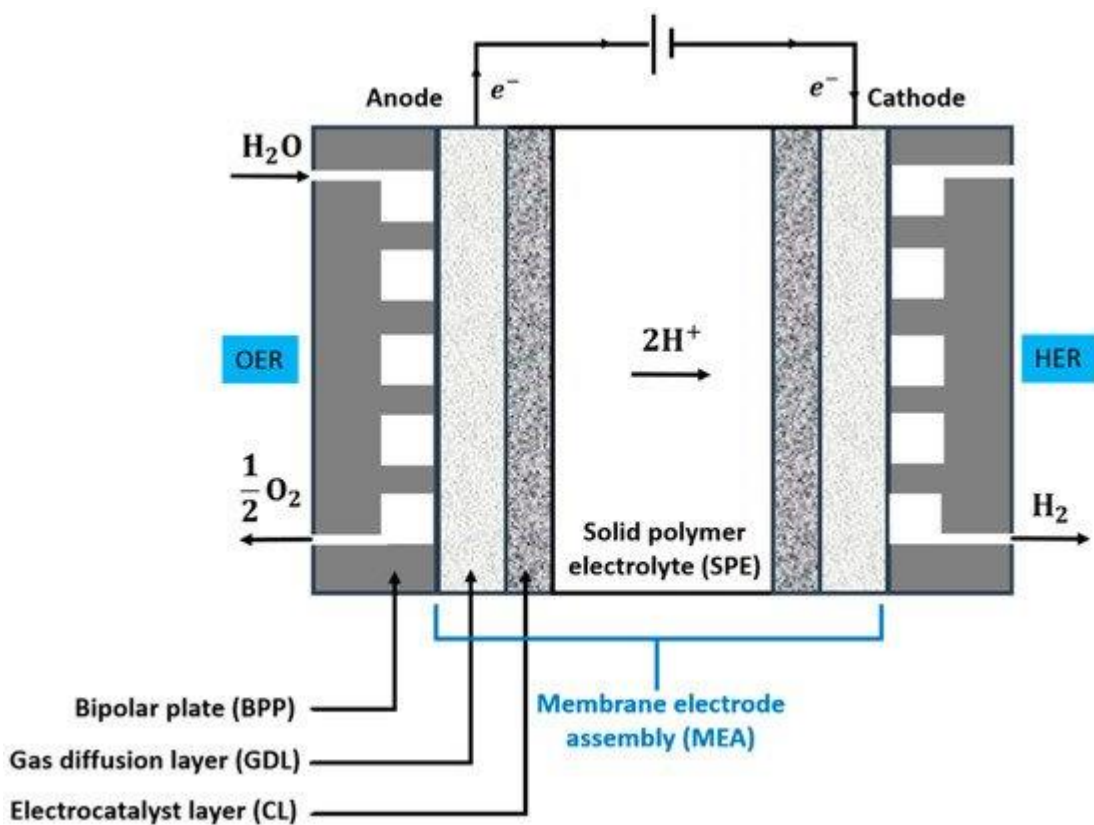
Figure 1.- Scheme of a single cell of a PEMWE. Taken from Ref. (10).
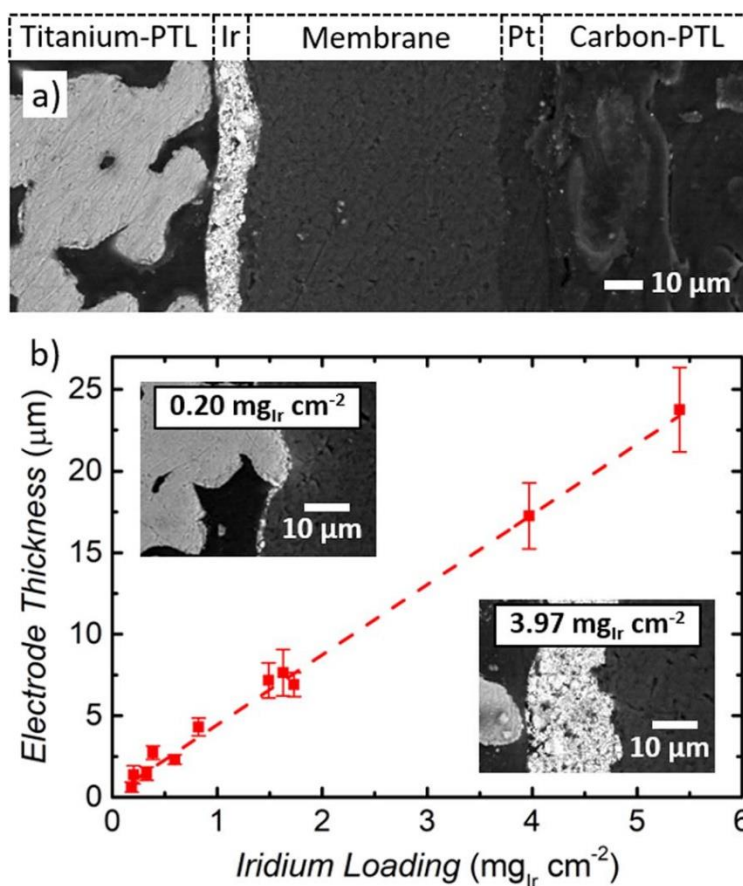
Figure 2.- a) SEM image of the cross-section of a MEA showing an IrO_2/TiO_2 + ionomer anode CL and a Pt/C + ionomer cathode CL, separated by a Nafion® 212 membrane. The anode and the cathode PTLs were made of Ti and carbon paper, respectively. b) Anode thickness as a function of the Ir loading, with two SEM cross-sectional pictures for different thicknesses as insets. Taken from Ref. (25).
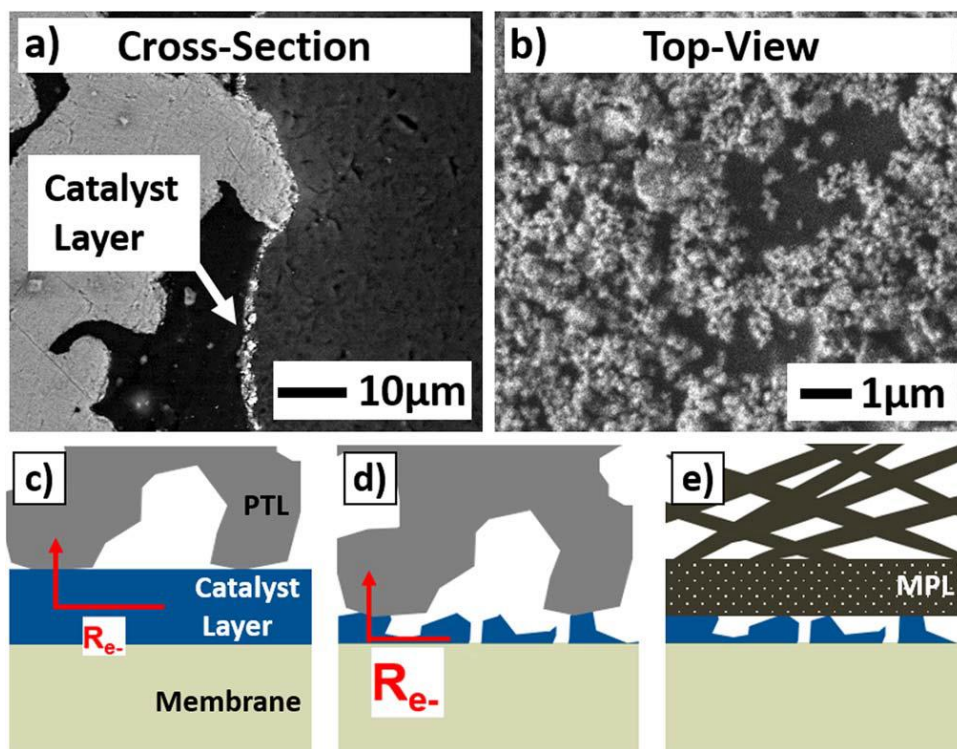
Figure 3.- a) Cross section and b) top-view SEM images of thin Ir-based CLs. The schemes illustrating the electronic transport between the Ti PTLs and the CLs are shown in c) for thick and d) thin CLs. In e), the Ti-based PTLs have been replaced by a carbon PTL with a MPL. Taken from Ref. (25).

\<Tables\>

Table I

Performance data of selected PEMWE single cells, made with different components, in the last years, under the indicated conditions. References sorted from the most recent.

Anode		Cathode		Operating conditions			Membrane	Degradation rate	Ref.
Catalyst	Loading (mg cm^{-2})	Catalyst	Loading (mg cm^{-2})	Voltage (V)	Current density (A cm^{-2})	T (ºC)			
Ir/IrO$_x$	0.3	Pt/C	0.2	2.09	1.8	50	Nafion® 211/Pt RL/Nafion® 117	24 µV/h, 1.8 A cm^{-2}, 3000 h	(84)
Ir@WO$_x$	0.14	70 wt% Pt/C	0.4	2.0	2.2	80	Nafion® 115	49.7 µV/h, 0.5 A cm^{-2}, 1030 h	(66)

IrO$_2$	1.40	60 wt% Pt/C	0.50	1.80	2.0	80	Nafion® D520	N/A	(15)
IrO$_2$	0.90	55.5-58.5 wt% Pt/C	0.25	1.80	3.6	80	Nafion® 212	N/A	(26)
RuO$_2$	3.0	30 wt% Pd/B$_3$-CNPs	0.70	1.86	0.50	80	Nafion® 115	2.04 V, 500 h (1 A cm^{-2})	(30)
Ir$_{0.7}$Ru$_{0.3}$O$_x$	0.40	40 wt% Pt/C	0.10	1.82	3.0	80	Aquivion® membrane (E98-09S)	90 µV/h 800 h	(69)
Ir/SnO$_2$:Sb	0.50 (Ir)	40 wt% Pt/C	1.0	N/A	N/A	N/A	Aquivion® membrane (E87-05S)	N/A	(60)
IrO$_2$	1.40	60 wt% Pt/C	0.50	1.80	1.1	80	Nafion® 117	200 h (2 A cm^{-2})	(22)
IrO$_2$/Sb-SnO$_2$ (7/3)	0.50	40 wt% Pt/C	5.00	1.70	~1.3	80	Nafion® 211	N/A	(100)

IrO_2 + Pt black (1:1)	0.92	Pt_{xAL}–PtFe/C	0.20	1.57	1.0	80	Nafion® 212	~70 µV h^{-1} 1 A cm^{-2} 1000 h	(46)
IrO_2	2.10	55.5-58.5 wt% Pt/C	0.40	1.80	6.0	80	N/A	N/A	(23)
IrO_2 (75%) /TiO_2	1.50-2.0 (Ir)	4.8 wt% Pt/C	0.025 (Pt)	1.79	3.6	80	Nafion® 212	N/A	(25)
IrO_2 (20%) /gCNH	N/A	Pt/C	4.0 (Pt)	1.80	~0.7	80	Nafion® 115	N/A	(88)
$IrRuO_x$	3.0	Pt black	0.086	1.80	~1.8	80	Nafion® 115	N/A	(31)
Ir black	2.0	Pt/C	1.0	1.80	~1.3	80	Nafion® N115/Pt (0.02 mg cm^{-2})/Nafion® NR212	190 µV h^{-1} (1 A cm^{-2})	(19)
IrO_2	2.50	40 wt% Pt/C	0.40	1.70	1.0	90	Nafion® 117	35.5 µV h^{-1}	(32)

40 wt% IrO$_2$/V-TiO$_2$ (20 at% V)	2.50	40 wt% Pt/C	0.50	1.80	0.6	80	Nafion® 117	N/A	(108)
Ir$_{0.7}$Ru$_{0.3}$O$_x$	1.0	40 wt% Pt/C	0.40	1.70	1.0	80	Nafion® NR212	81 µV h^{-1}	(70)
IrO$_2$/Ti (50 wt% Ti)	0.1	46 wt% Pt/C	0.25	1.73	1.0	80	Nafion® NRE 115CS	1000 h 20 µV h^{-1}	(105)
Ru@Pt (core-shell)	0.10	Pt@WO$_3$ (core-shell)	0.10	1.80	1.0	80	Nafion® 117	N/A	(61)
IrO$_2$/Sb-SnO$_2$ nanowire	0.75	40 wt% Pt/C	0.20	1.62	2.0	80	Nafion® NR212	0.76 mV h^{-1} (0.45 A cm^{-2} at 35 ºC)	(117)
67 wt% IrO2/Ti$_n$O$_{2n-1}$	1.0	30 wt% Pt/Vulcan XC-72	1.0	1.80	0.700	80	Nafion® 115	N/A	(116)